Carbohydrate Polymers 97 (2013) 188–195

Contents lists available at SciVerse ScienceDirect

Carbohydrate Polymers

journal homepage: www.elsevier.com/locate/carbpol

An interpenetrating HA/G/CS biomimic hydrogel via Diels–Alder click chemistry for cartilage tissue engineering

Feng Yu[a,b], Xiaodong Cao[a,c,*], Lei Zeng[a,c], Qing Zhang[a,b], Xiaofeng Chen[a,b,c,*]

[a] School of Materials Science and Engendering, South China University of Technology, Guangzhou 510641, PR China
[b] National Engineering Research Centre for Tissue Restoration and Reconstruction, Guangzhou 510006, PR China
[c] Guangdong Province Key Laboratory of Biomedical Engineering, South China University of Technology, Guangzhou 510640, PR China

ARTICLE INFO

Article history:
Received 26 October 2012
Received in revised form 3 January 2013
Accepted 12 April 2013
Available online 26 April 2013

Keywords:
Gelatin
Hyaluronic acid
Chondroitin sulfate
Interpenetrating hydrogel
Diels–Alder click chemistry

ABSTRACT

In order to mimic the natural cartilage extracellular matrix, a novel biological degradable interpenetrating network hydrogel was synthesized from the gelatin (G), hyaluronic acid (HA) and chondroitin sulfate (CS) by Diels–Alder "click" chemistry. HA was modified with furylamine and G was modified with furancarboxylic acid respectively. ^{1}H NMR spectra and elemental analysis showed that the substitution degrees of HA-furan and G-furan were 71.5% and 44.5%. Then the hydrogels were finally synthesized by cross-linking furan-modified HA and G derivatives with dimaleimide poly(ethylene glycol) (MAL-PEG-MAL). The mechanical and degradation properties of the hydrogels could be tuned simply through varying the molar ratio between furan and maleimide. Rheological, mechanical and degradation studies demonstrated that the Diels–Alder "click" chemistry is an efficient method for preparing high performance biological interpenetrating hydrogels. This biomimic hydrogel with improved mechanical properties could have great potential applications in cartilage tissue engineering.

1. Introduction

Treatment of articular cartilage injury has been a challenge for a long time in musculoskeletal medicine due to the poor intrinsic regeneration capacity. Current clinical methods of repairing defective cartilage include autologous chondrocyte implantation (ACI), mosaicplasty, and microfracture, all of which are limited in their capabilities of regenerating cartilage with normal composition and proper mechanical properties to achieve the functional recovering (Chung & Burdick, 2008). Because of lack of efficient treatment modalities, development of cartilage tissue engineering has attracted more and more attention (Toh, Spector, Lee, & Cao, 2011). Great effects have been put into cartilage regeneration research to develop a system with mechanical properties and biological functions close to native tissue and a relatively fast restoration of tissue functions. As we know, hydrogel is increasingly becoming an important scaffold in the fields of cartilage tissue engineering because of the water swollen network and the suitable delivery capacity of cells and bioactive agents (Cheung, Lau, Lu, & Hui, 2007). Cells can be suspended and their round shape will be retained in the 3 dimensional structure of hydrogels which are required to avoid the undesired dedifferentiation of chondrocytes during cultured in vitro and in vivo. In addition, hydrogel is capable of transducing mechanical loads to control forces on encapsulated cells, which is similar to physiological conditions (Appelman, Mizrahi, Elisseeff, & Seliktar, 2011; Cheung et al., 2007; Chung & Burdick, 2008; Steward, Liu, & Wagner, 2011).

In the field of cartilage tissue engineering, the hydrogels are generally divided into at least two categories based on their compositional differences. (I) The pure natural biomaterials, which are further, distinguished as protein-based (collagen, fibrin and gelatin) and polysaccharide-based (hyaluronic acid, chitosan, agarose and alginate) biomaterials (Vinatier, Mrugala, Jorgensen, Guicheux, & Noel, 2009). The advantage of employing these materials is that the natural bodily constituents can provide a natural adhesive surface for cells and can carry the required information for their activities as well. Furthermore, the degradation products are physiological and non-toxic (Stoop, 2008). Unfortunately, the application of these materials is limited as they usually have a relatively poor mechanical performance and degrade at an undesired fast speed. Nimmo et al. had prepared hyaluronic acid hydrogels that have a complete degradation in less two days in PBS with 50 U/mL of hyaluronidase (Nimmo, Owen, & Shoichet, 2011). Other natural hydrogels usually have the similar problems in cartilage tissue engineering (Crescenzi, Cornelio, Di Meo, Nardecchia, & Lamanna, 2007; Hu, Li, Zhou, & Gao, 2011; Palumbo et al., 2012;

* Corresponding authors at: School of Materials Science and Engendering, South China University of Technology, Guangzhou 510641, PR China.
Tel.: +86 20 22236066; fax: +86 20 87111752.
E-mail addresses: caoxd@scut.edu.cn (X. Cao), chenxf@scut.edu.cn (X. Chen).

0144-8617/$ – see front matter © 2013 Elsevier Ltd. All rights reserved.
http://dx.doi.org/10.1016/j.carbpol.2013.04.046

Tan, Rubin, & Marra, 2011). (II) Combination of synthetic polymers and natural biomaterials (Vinatier et al., 2009). These composite hydrogels spring out to resolve the limitations of natural hydrogels which were mentioned previously. However, the introduction of synthetic polymers inevitably leads other challenges including the potential increase in local pH caused by the acidic degradation products, the excessive inflammatory responses and the poor clearance and chronic inflammation associated with the use of high molecular weight polymers (Stoddart, Grad, Eglin, & Alini, 2009; Stoop, 2008; Temenoff & Mikos, 2000).

In order to improve the relatively poor degradation and mechanical properties of the natural hydrogels, an interpenetrating hydrogel was fabricated to mimic the cartilage compositions by Diels–Alder click chemistry in present work. The methods applied in the designing and fabrication of hydrogels have been developed dramatically by the utilization of click chemistry, a concept introduced by Sharpless and co-workers in 2001 (Yigit, Sanyal, & Sanyal, 2011). Compared to previous traditional chemistry and physical cross-linking methodologies, Click chemistry possesses advantages such as high yields under mild conditions, high specificity, selectivity, and no offensive byproducts as well (Clark & Kiser, 2009; Kolb, Finn, & Sharpless, 2001; Tasdelen, 2011; Yigit et al., 2011). The common types of click chemistry include azide-alkyne [3+2] cycloaddition, thiol-alkene addition reaction which both catalyzed by (Cu) (I) and the furan-maleimide [4+2] Diels–Alder (DA) cycloaddition. Since the catalyst (Cu) (I) has known micro-molar toxicityand must be washed out of the gel prior to the exposure to cells (Clark & Kiser, 2009), the Diels–Alder cycloaddition without catalyst has generated significant interests (Tasdelen, 2011). Great deals of work on utilization of Diels–Alder reaction to build up the synthetic polymer hydrogels have been carried out (Liu, Hsieh, & Chen, 2006; Wei et al., 2010; Wei, Yang, Zheng, & Shen, 2009). However, there are very few reports on using Diels–Alder reaction to prepare interpenetrating hydrogels for cartilage tissue engineering (Tasdelen, 2011).

Hence, in this study, Diels–Alder reaction was selected to fabricate hydrogel to achieve an interpenetrating natural hydrogel with improved performances. In addition, the hydrogels were synthesized with hyaluronic acid, gelatin and chondroitin sulphate, which are the main components in ECM of cartilage tissue. Hyaluronic acid (HA) is a linear high-molecular weight polysaccharide. It is the backbone of glycosaminoglycan (GAG) superstructure complexes, mostly associated with other polysaccharides such as chondroitin sulphate (Kogan, Šoltés, Stern, & Gemeiner, 2006). Due to its good biocompatibility, biodegradability, as well as excellent gel-forming properties, hyaluronic acid shows potential application in biomedical hydrogel systems. Hyaluronic acid can be oxidized and generate reactive aldehyde functions, which can develop chemical crosslinking action with amino functions via Schiff's base linkage (Itoa et al., 2007; Ruhela, Riviere, & Szoka, 2006). It has been proved that HA hydrogels can not only support and maintain chondrocyte viability and phenotype when cultured in vitro and in vivo, but also support and promote the chondrogenic differentiation of MSCs (Chung, Erickson, Mauck, & Burdick, 2008; Chung, Mesa, Randolph, Yaremchuk, & Burdick, 2006; Matsiko, Levingstone, O'Brien, & Gleeson, 2011). In native cartilage EMC, collagen is a fibrous molecule that resist shear stresses in the superficial zone, distribute the load throughout the tissue in the middle zone and resist compressive forces in the deep zone (Klein, Malda, Sah, & Hutmacher, 2009). Gelatin (G) is a natural biopolymer derived from partial hydrolysis of native collagen and in which there are many integrin-binding sites for cell adhesion and differentiation (Lee et al., 2008). Chondroitin sulphate (CS) is a predominant component of ECM and it is known that chondroitin sulfate can promote cell secretion of type II collagen and glycoproteins (Chang et al., 2006).

The hybrid HA/G/CS bionic interpenetrating hydrogel has been prepared in aqueous solution at a mild temperature of 37 °C. The morphology, structural, viscoelasticity, mechanical properties, swelling and degradation rate of the interpenetrating hydrogels were carefully investigated.

2. Materials and methods

2.1. Materials

Hyaluronic acid sodium (molecular weight 1×10^6) was purchased from Shanghai crystal pure industrial Co., Ltd. (Shanghai, China). Gelatin, 1-ethyl-3-(3-dimethylaminopropyl) carbodiimide hydrochloride (EDC), N-hydroxysuccinimide (NHS), 2-morpholinoethane sulfonic acid (MES), 4-(4,6-dimethoxy-1,3,5-triazin-2-yl)-4-methylmorpholinium chloride (DMTMM), furylamine, furancarboxylic acid, chondroitin sulfate and hyaluronidase were purchased from Sigma–Aldrich (Guangzhou, China). Dimaleimide poly(ethylene glycol) (MAL-PEG-MAL) (molecular weight 2×10^3) was purchased from Shanghai Sunway Pharmaceutical Technology Co., Ltd. (Shanghai, China). Other chemicals were of analytical grade and used as received.

2.2. Synthesis

2.2.1. Synthesis and characterization of HA-furan (Scheme 1)

HA-furan was prepared by amidation of the carboxyl groups of HA with the amine groups of furylamine. Briefly, HA (500 mg, 1.25 mmol carboxyl groups) was dissolved in 100 mL of MES buffer (100 mM, pH 5.5), in which DMTMM (1.384 g, 5 mmol) was added to active the polysaccharide carboxyl groups. Subsequently, furylamine (220 μL, 2.5 mmol) was added dropwise by using a pipette, and keep stirring at room temperature for 24 h. After that, it was dialyzed against distilled water for 5 days (M_w cut-off 1.4×10^4). Finally, HA-furan derivative was obtained as a white porous sponge by lyophilization. The degree of substitution (DS) was determined from ^{1}H NMR (Bruker AVANCE 400 MHz) spectra (Nimmo et al., 2011).

2.2.2. Synthesis and characterization of G-furan (Scheme 2)

500 mg of EDC and 300 mg of NHS were added to 100 mL of 1% gelatin solution (about 0.5 mmol amino) with 30 min magnetic stirring. After adding the furancarboxylic acid (140 mg, 1.25 mmol) into the solution, the reaction was maintained for 24 h at room temperature. Subsequently, the resulting mixture was sealed in a semi-permeable membrane bag with a molecular weight cut-off 1.4×10^4 Da for dialyzing over 5 days. After that, G-furan derivative as a white porous sponge was obtained by lyophilization. The structure of G-furan was confirmed by the new peaks of 6.45, 6.90, and 7.50 ppm (furan protons) in ^{1}H NMR spectra. The degree of substitution (DS) was derived from C and N contents that were determined by elemental analysis (Eager 300) (Hu, Zhou, Zhang, Tan, & Gao, 2008):

$$R(\mathrm{C/N\ molar\ ratio}) = \frac{\mathrm{C}/12}{\mathrm{N}/14} \quad (1)$$

$$\mathrm{DS} = \frac{(R_{\mathrm{G\text{-}furan}} - R_{\mathrm{Gelatin}}) \times 31}{4} \times 100\% \quad (2)$$

2.2.3. The formation of HA/G pre-hydrogel (Pre-H) (Scheme 3)

HA/G pre-hydrogel was synthesized by reacting HA-furan and G-furan with MAL-PEG-MAL cross-linker in MES buffer (100 mM, pH 5.5). HA-furan (45 mg) and G-furan (30 mg) were mixed in 3 mL of MES buffer. The concentrations of HA-furan and G-furan were held at 1.5% and 1% w/v respectively, and the concentration

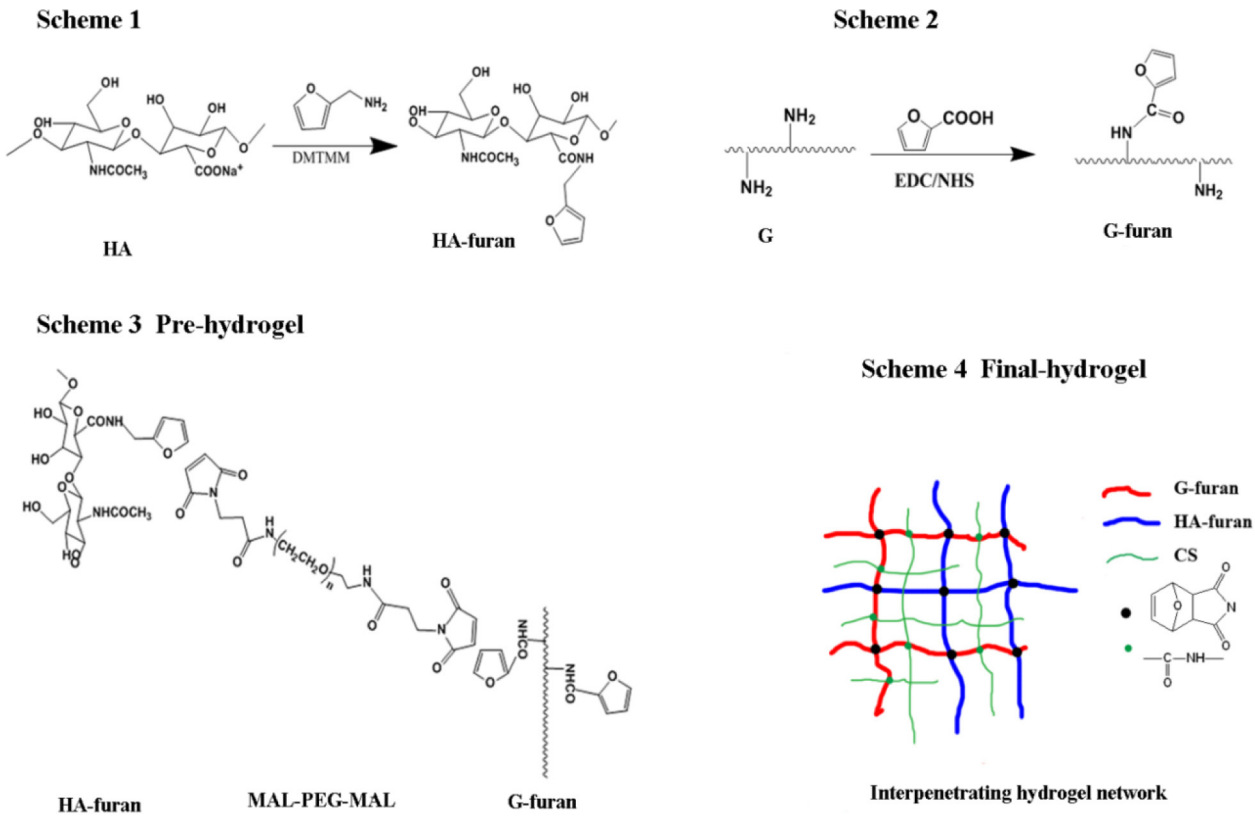

Schemes 1–4. Schematic representation of the formation of interpenetrating hydrogels by Diels–Alder click chemistry and EDC/NHS cross-linking.

of MAL-PEG-MAL was varied to examine differences in hydrogel properties. The mole ratio (MR) of furans to maleimide was ranged from 5:1, 10:1 to 20:1, which was presented as MR5, MR10, and MR20 respectively. The mixture solution of HA-furan and G-furan were divided into three text tubes and each of them was of 1 mL. MAL-PEG-MAL (54 mg, furan:maleimide = 5:1 (MR5); 27 mg, furan:maleimide = 10:1 (MR10); 13.5 mg, furan: maleimide = 20:1 (MR20)) was separately dissolved in 375 μL MES buffer, and then added to three text tubes. The Diels–Alder reaction was carried out at 37 °C overnight.

2.2.4. The formation of HA/G/CS interpenetrating hydrogels (Final-H) (Scheme 4)

After freeze-drying, the HA/G pre-hydrogels were immersed into MES buffer solution (100 mM, pH 5.5) containing chondroitin sulfate to get HA/G/CS interpenetrating hydrogels. Briefly, the cross-linked HA/G pre-hydrogel sample (200 μL), which was prepared in pore plate according to the above procedure, was immersed into chondroitin sulfate MES buffer (2 mL, 1% w/v) containing EDC (20 mg) and NHS (13.3 mg) and then put in shake bed at 37 °C for 24 h.

2.3. Characterization of Pre-H and Final-H

2.3.1. The morphology of hydrogel

In order to observe the morphology of hydrogel network, the hydrogels were lyophilized overnight to obtain scaffolds. Subsequently, the scaffolds were immersed into liquid nitrogen and cut off immediately. The cross-section of the scaffolds was observed using a scanning electron microscope (SEM) (Quanta 200, Netherlands FEI) after being gold-coated in a sputter coater (Sanyo Denshi, Japan).

2.3.2. Viscoelasticity characterization

Rheological measurements on the hydrogels (25 mm in diameter, 2.5 mm in height) were performed using a strain-controlled rheometer (TA ARES-RFS) with a parallel plate. The diameter of the plate is of 25 mm and the gap distance is of 1 mm respectively. The frequency sweep was conducted from 0.1 to 100 rad/s at 1% strain to determine the shear elastic modulus (G') and loss modulus (G'') of the hydrogels. All tests were carried out at 37 °C.

2.3.3. Compressive modulus

Compressive modulus of elasticity was measured using a dynamic mechanical analyser (ELF3200, Endura TEC) with unconfined compression mode at a constant stress rate of 40 mN/min at 37 °C.

2.3.4. Equilibrium swelling

To examine the swelling properties, cross-linked hydrogel samples (200 μL) were prepared in a pore plate according to above procedure. The samples were immersed into the PBS (100 mM, pH 7.4) at 37 °C for 48 h until the equilibrium of swelling had been reached. The swollen hydrogels were weighed with a microbalance quickly after the excess of water on the surfaces was absorbed with a filter paper. The swelling ratio was calculated using the following equation:

$$\mathrm{SW} = \frac{W_s - W_d}{W_d} \quad (3)$$

where W_s and W_d are the weights of the hydrogels at equilibrium swelling state and freeze-dried state, respectively.

2.3.5. Degradation assay

To determine the stability, we synthesized hydrogel samples (200 μL) in a pore plate according to above procedure and allowed them to swell in PBS (100 mM, pH 7.4) for 48 h at 37 °C, after which

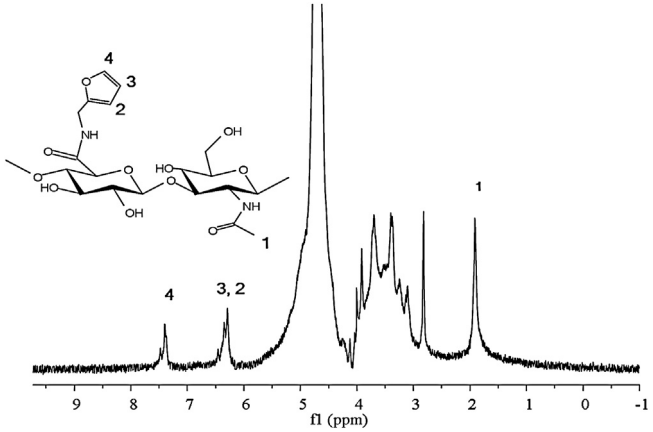

Fig. 1. ^{1}H NMR spectra in D_2O (400 MHz) of HA-furan (DS = 71.5%). Degree of substitution was determined by comparing the integrated areas under the proton peaks at 6.26, 6.46, and 7.65 ppm (furan protons), indicated by 2, 3, and 4 to that of the peak at 1.9 ppm (N-acetyl glucosamine of HA), indicated by 1.

the mass of the samples were measured (M_s). Degradation experiments were performed using 50 U/mL of hyaluronidase in PBS at 37 °C. At the selected time points, the hydrogels were weighed (M_t) quickly after removing the supernatant, and the percent of hydrogel mass remaining relative to the original swollen mass was calculated (M_t/M_s). Fresh buffer containing hyaluronidase was replaced at each time point. As a control, the degradation profiles were also recorded for hydrogels incubated in PBS without enzyme at 37 °C.

3. Results and discussion

3.1. Synthesis and characterization of HA and G derivatives

HA-furan derivative was prepared in one-step reaction by coupling furfurylamine to HA using DMTMM reagent (see Scheme 1). DMTMM has been recognized as a highly efficient activator of polysaccharide carboxyl groups in aqueous conditions, superior to traditional carbodiimide coupling. The chemical structure and degree of substitution (DS) were confirmed by ^{1}H NMR (Fig. 1). Resonances at 6.26, 6.46, and 7.65 ppm verified the presence of furan protons, and their integrated ratios were compared with that

Table 1
Basic parameters of gelatin and sodium hyaluronate before and after modification.

Sample	C content	N content	C/N mole ratio	DS
Gelatin	41.93	15.33	3.19	–
G-furan	43.67	15.62	3.25	44.5%
HA	33.41	2.929	13.307	–
HA-furan	39.64	9.352	4.945	70.9%

of the N-acetyl glucosamine proton peak of native HA, appearing at 1.9 ppm. According to the area ratio, the DS of HA-furan was determined to be of 71.5%. It also can be obtained from the C and N contents according to the elemental analysis (Table 1).

G-furan derivative was prepared by coupling furancarboxylic acid to G using EDC and NHS reagent (see Scheme 2). The DS of G-furan is 44.5%, which was quantified from the C and N contents according to the basic parameters of elemental analysis (Table 1). In the spectra of ^{1}H NMR (Fig. 2), the new peaks at 7.50, 6.90 and 6.45 ppm correspond to the protons of the furan ring. The relatively high DS of HA-furan and G-furan will have a good effect on the cross-linking process.

3.2. Synthesis and structure of Pre-H and Final-H

The hydrogels with three different cross-linking densities were prepared. When the mole ratio of furan to maleimide was MR20, however, the resulted product is too weak to be an intact hydrogel. Therefore, the hydrogels with MR5 and MR10 were finally synthesized and their properties were carefully studied. The morphology of hydrogels with different furan to maleimide ratios were shown in Fig. 3(e). It is a hyaline elastomer and looks like native cartilage. The SEM images of freeze-dried Pre-H and Final-H with MR5 and MR10 were shown in Fig. 3(a) and (c), and (b) and (d). The freeze-dried scaffolds exhibited a uniform pore size and good connectivity. The pore size of MR5 ranged from 150 to 250 μm in Pre-H and 100 to 150 μm in Final-H. In Fig. 3(c), it was obviously showed that the pores were smaller than that in Fig. 3(a), and partly covered by the chondroitin sulfate due to the second interpenetrating reaction. The same phenomenon can be also observed in the Pre-H and Final-H with MR10. The pore size of MR10 in Pre-H was 400–600 μm, which was larger than MR5 due to the less cross-linked points (Fig. 3(b)). Similarly, the Final-H of MR10 also had

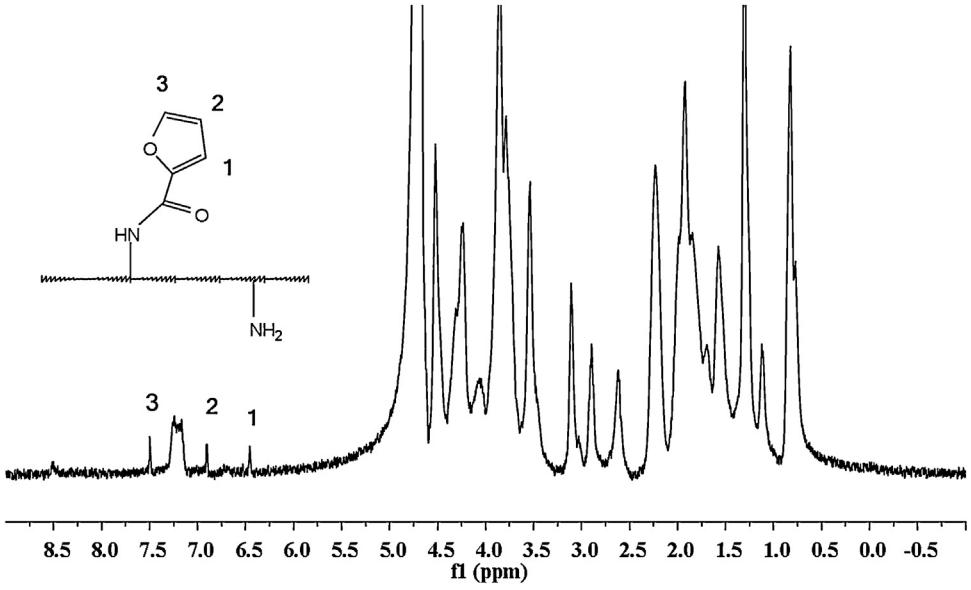

Fig. 2. ^{1}H NMR spectra in D_2O (400 MHz) of G-furan. The peaks at 6.45, 6.90, and 7.50 ppm were indicated by 1, 2, and 3 respectively.

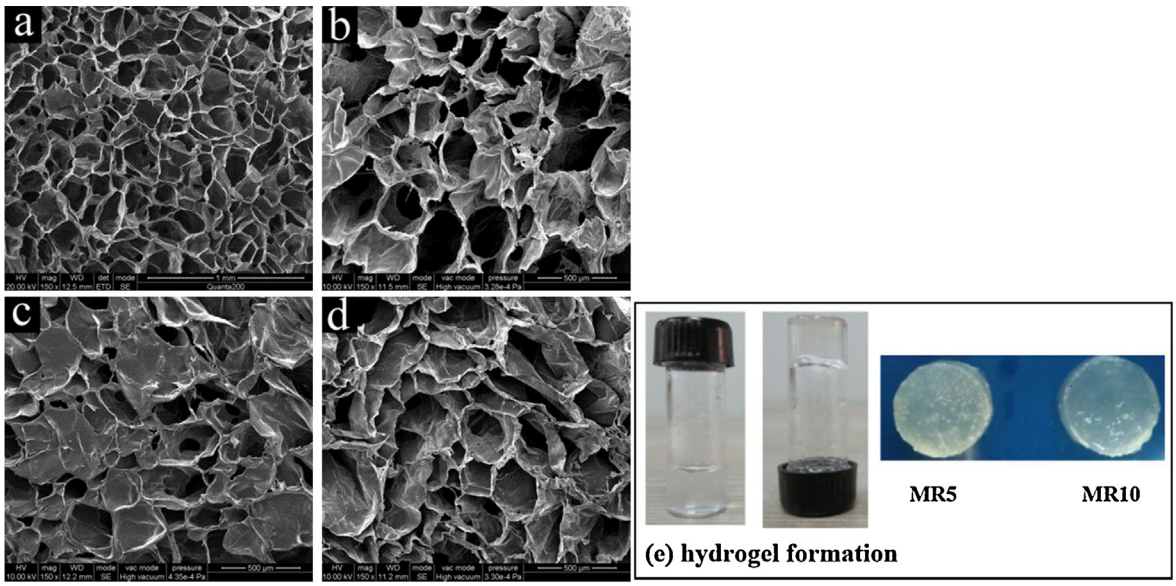

Fig. 3. SEM of Pre-H and Final-H with different furan to maleimide ratio. (a) Pre-H with MR5, (c) Final-H with MR5, (b) Pre-H with MR10, (d) Pre-H with MR10. (e) Morphology of hydrogels with MR5 and MR10.

a smaller pore size of 250–400 μm than that of Pre-H. There was a contractive phenomenon after lyophilization in both networks. Some studies have demonstrated that the pore size and the pore interconnection play an important role in cell seeding, nutrient transport and cell migration during the cell culturing phase. Silva et al. had reported that large pores (250–500 μm) induced the cell proliferation, production of proteoglycans and collagens, while small pores (65–125 μm) enhanced the proteoglycan deposition (Alves da Silva et al., 2010). Lu et al. showed that the large pore interconnections promoted nutrient transport and metabolic product outflow for cell proliferation (Lu et al., 1999). In this work, the pore size of HA/G/CS biomimic hydrogel can be mediated from small to large pores simply by varying the cross-linking density. The additional experimental results showed that when the mole ratio of furan to maleimide was controlled to MR8, the pore size of 200–350 μm. Therefore, we predicted that we can obtain one kind of pore size that not only induce cell proliferation and production of collagens, but also the proteoglycan deposition.

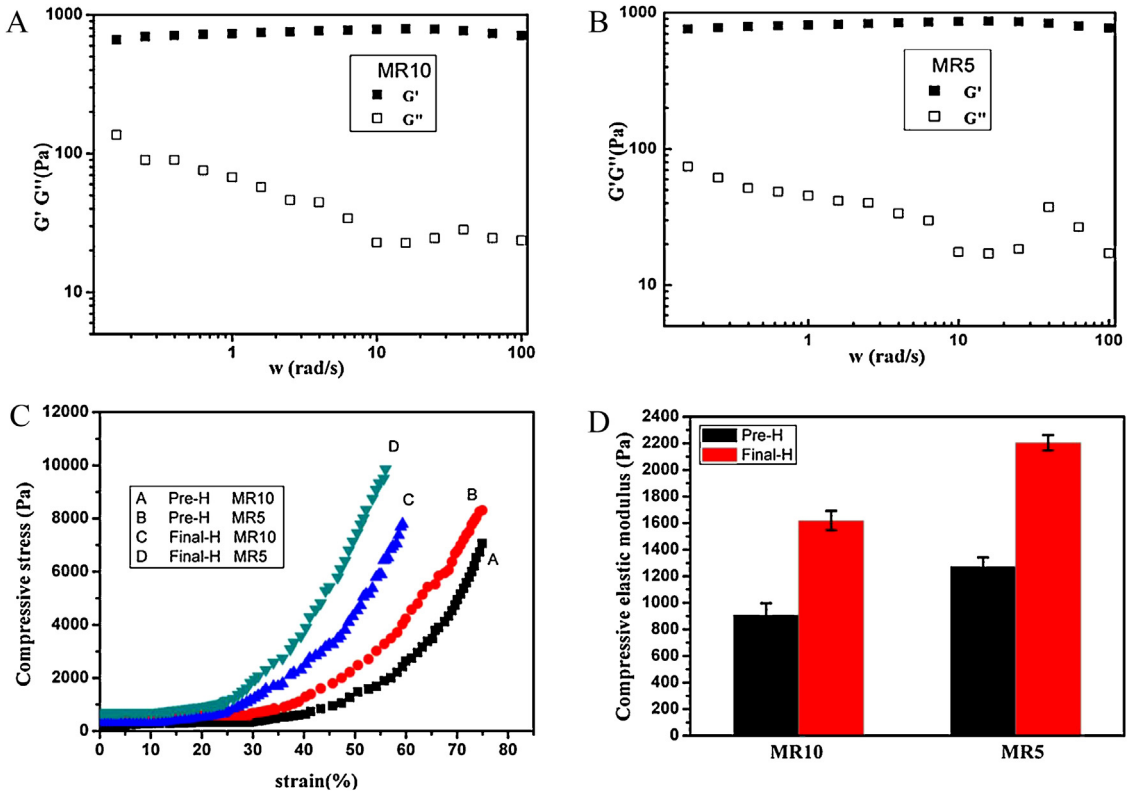

Fig. 4. The mechanical properties of hydrogels. (a) Rheological characterization of Pre-H with MR10. (b) Rheological characterization of Pre-H with MR5. (c) Compressive stress–strain curve of hydrogels with different furan to maleimide ratio. (d) Compressive elastic modulus of hydrogels.

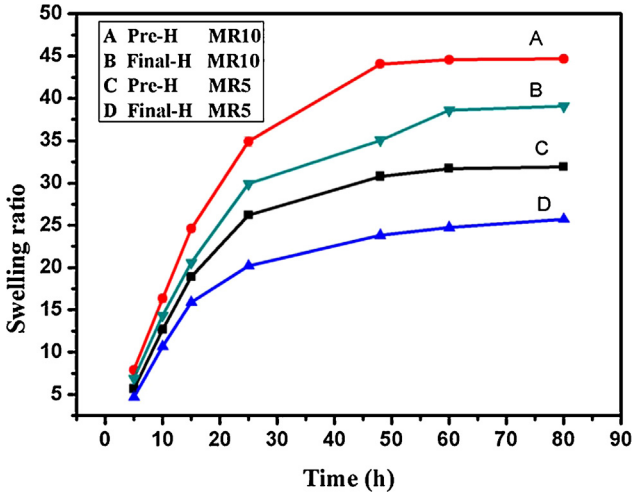

Fig. 5. The swelling properties of hydrogels.

3.3. Mechanical properties

The elastic properties of Pre-H and Final-H with different furan to maleimide ratio were characterized by rheology studies using parallel plate geometry at 37 °C. The storage modulus G', loss modulus G'' and the shear elastic modulus of the pre-hydrogel were shown in Fig. 4(a) and (b). G' was constant within the frequency range used in our study, which indicates that hydrogel was cross-linked prior to measure. Hydrogels were analyzed corresponding to their furan/maleimide molar ratio, which is their cross-linker concentration. In all experiments, the furan concentration was held constant while the maleimide concentration was varied. Cross-linker concentration was altered to distribute either MR5 or MR10 within hydrogels. As shown in Fig. 4(a) and (b), the shear elastic modulus of the hydrogels increased with higher cross-linker concentration. There was a significant difference between all hydrogel formulations ($p < 0.001$) where increased maleimide concentrations resulted in higher cross-linking density. Accordingly, the Pre-H of MR10 owned a G′value of 714 ± 31 Pa, while MR5 owned a G′value of 862 ± 38 Pa. It indicated that MR5 gel was stiffer than MR10, which was in an agreement with the results of compression testing showed in Fig. 4(d). The results are much better than that of HA hydrogels reported in other literatures, in which the G′ were all below 600 Pa (Hu et al., 2011; Nimmo et al., 2011; Tan et al., 2011). We can also see that the storage modulus G' was almost two orders of magnitude higher than G'' in both MR10 and MR5, suggesting that they were strong gels with less viscous properties (Zhou & Wu, 2011; Zhou, Wu, Yue, & Zhang, 2011).

Fig. 4(c) shows the compressive stress-strain curve of hydrogels with different furan to maleimide mole ratio. As can we see, in two different ratios, Final-H could sustain much higher stress than Pre-H, especially at high strain levels. MR5 hydrogel was more rigid and stronger than MR10 in both Pre-H and Final-H. This behavior can be ascribed to the higher cross-linking density. The compressive elastic modulus (E) was calculated by the following equation (Munic & Geustens, 2001; Zhou et al., 2011):

$$\sigma = E(\lambda - \lambda^2) \quad (4)$$

where λ is the relative deformation of the specimens. As the initial surface of the cylindrical sample was not perfectly flat, the strain from 10% to 15% was used to determine the value of E (Buyanov, Gofman, Revel'skaya, Khripunov, & Tkachenko, 2010). The results calculated were shown in Fig. 5(d). The E of MR5 were of 1273 ± 69 Pa, 2204.6 ± 58 Pa, while MR10 were of 909 ± 88 Pa, 1618.5 ± 73 Pa in Pre-H and Final-H, respectively. The tendency of elastic modulus of hydrogels is in agreement with that of shear storage modulus. Jha et al. had prepared a hyaluronic acid-based hydrogel matrices which with a great increasing elastic modulus via the covalent integration of microgel into networks (Jha, Malik, Farach-Carson, Duncan, & Jia, 2010). The results show that mechanical properties of HA/G/CS hydrogels are comparable with the reinforced hydrogel.

3.4. Swelling rate

The swelling behavior of these hydrogels was probed gravimetrically by recording the water uptake by the hydrogels over time until they reached equilibrium. As shown in Fig. 5, both MR5 and MR10 hydrogels swelled rapidly and reached swelling equilibrium within 48 h. According to the equation $SW = (W_s - W_d)/W_d$, which mentioned in the Section 2, we have calculated the equilibrium swelling rate of MR5 and MR10. It was observed that an increase of the cross-linkers concentration led to a decrease in the swelling capacity of the hydrogel. The equilibrium swelling rate of MR5 was 31.72 ± 0.47 in Pre-H and 25.72 ± 0.53 in Final-H, which were lower than that of MR10 (44.06 ± 0.84 in Pre-H and 39.06 ± 0.77 in Final-H). This behavior could be contributed to the increase in the concentration of hydrophilic cross-linkers within the hydrogel matrix and the tough cross-linked network obtained. It is well known that the swelling properties of hydrogels mainly depend on the hydrophilic ability of the functional groups and the effective crosslink density of the hydrogels (Tamura et al., 2012). For the two different hydrogels, the MR5 owned the higher concentration of hydrophilic functional groups of hydroxyl and higher crosslinking density. On the one hand, the water was brought into the network through the hydrogen bonds formed by water and the hydrophilic hydroxyl group (Liu, Xu, Guo, & Han, 2009; Tominaga et al., 2012). On the other hand, the higher chemical cross-linked network restricted the water to permeate. The results showed that MR5 had the lower swelling capacity than MR10, indicating that the chemical crosslinking density played a more important role in swelling property in this work.

3.5. Degradation assay

To monitor degradation of hydrogels in vitro, samples were incubated in PBS with 50 U/mL of hyaluronidase and PBS only at 37 °C. Their masses were recorded over 21 days. As shown in Fig. 6, both of the samples incubated in PBS (controls) showed no significant mass loss after 21 days. It is because there were no reagents or enzymes that could cause the network broken in PBS buffer solution. The hydrogel network kept complete and restrained degradation in 21 days. But, the network would become more swelled and disband at last along with the time went (Tang, Sun, Fan, & Zhang, 2012; Toh, Lim, Kurisawa, & Spector, 2012). Whereas the samples incubated in hyaluronidase were completely degraded in this time frame. The degradation rate directly correlated with the cross-linker concentration and enzyme content. In the present of the hyaluronidase, the chain of hyaluronic acid would be broken. The breakage of the sodium hyaluronate backbones lead to the partly dismissing of hydrogel network (Rice, Homier, Waters, & Anseth, 2008; Sun et al., 2012). Meanwhile, the water and enzyme were easier to penetrate into the network and cause the large area of degradation. Meanwhile, the crosslinking density also played an important role in the degradation process. The higher density can restrain the damage of network, while the lower density can contribute the rate of degradation. As shown in Fig. 6, the remained hydrogel mass of MR10 was less than 40% in pre-hydrogel within 10 days. However, that of MR5 was more than 40% in both Pre-H and Final-H even within 15 days. Because physiological hyaluronidase levels are much lower than that used in this study, it

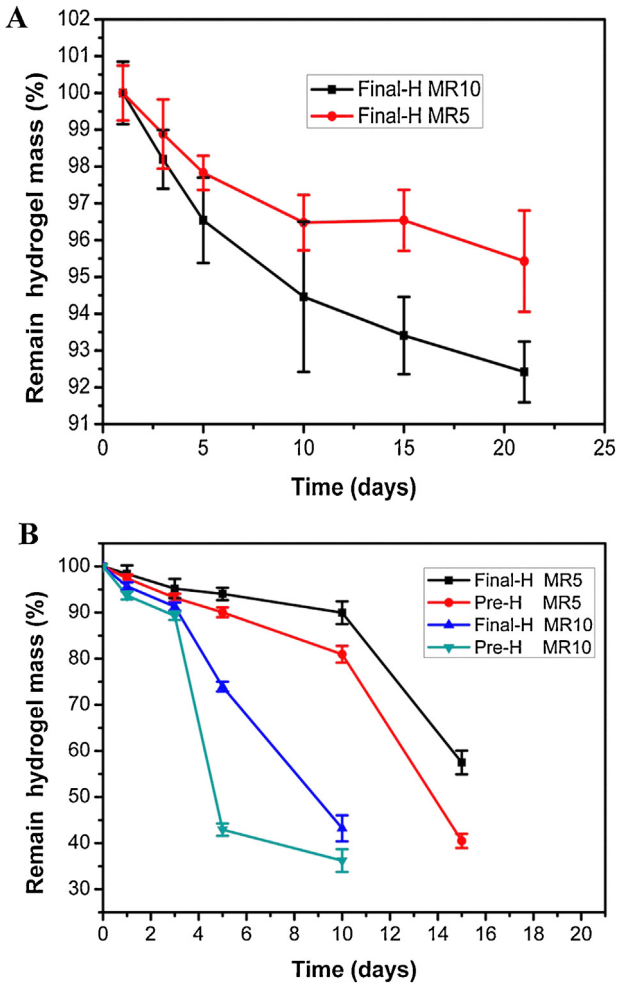

Fig. 6. Degradation rate of hydrogels. (a) The degradation rate of Final-H in PBS. (b) The degradation rate of Pre-H and Final-H in PBS with hyaluronidase.

could be predicted that the degradation rates for interpenetrating hydrogels would be much slower in vivo (Nimmo et al., 2011). These results suggested that a sufficient cross-linking efficiency for Diels–Alder interpenetrating hydrogels was obtained in this work.

4. Conclusion

Diels–Alder click chemistry and EDC/NHS crosslinking reaction are efficient cross-linking methods to prepare interpenetrating hydrogels. HA-furan and G-furan were achieved in one step reaction and had high substitution degree. The hydrogel was obtained requiring neither additional organic cross-linking agents nor catalysts, which result in clean and non-toxic materials. Hydrogels with different cross-linking degree have been characterized and proved that hydrogels with different ratios have good mechanical, swelling, degradation properties, which are suitable in soft tissue engineering. The Final interpenetrating hydrogels have better performance than the pre-hydrogels. Hopefully this biodegradable bionic hydrogel can serve as a therapeutically platform for cartilage tissue engineering applications. A series of following work about cell culture will be done to detect chondrocyte cytoactive and metabolic behavior in this bionic hydrogel scaffolds.

Acknowledgments

This work was financially supported by National Basic Research Program of China (973 Program) (Grant No. 2011CB606204, 2012CB619100), Key Program of the National Natural Science Foundation of China (Grant No. 50830101), National Natural Science Foundation of China (Grant No. 51172073, 51072055), Fundamental Research Funds for the Central Universities (Grant No. 2012ZP0001), Program for New Century Excellent Talents in University (NCET-11-0148) and the Specialized Research Fund for the Doctoral Program of Higher Education of China (Grant No. 20110172120002).

References

Alves da Silva, M. L., Crawford, A., Mundy, J. M., Correlo, V. M., Sol, P., Bhattacharya, M., et al. (2010). Chitosan/polyester-based scaffolds for cartilage tissue engineering: Assessment of extracellular matrix formation. *Acta Biomaterialia*, *6*(3), 1149–1157.

Appelman, T. P., Mizrahi, J., Elisseeff, J. H., & Seliktar, D. (2011). The influence of biological motifs and dynamic mechanical stimulation in hydrogel scaffold systems on the phenotype of chondrocytes. *Biomaterials*, *32*(6), 1508–1516.

Buyanov, A. L., Gofman, I. V., Revel'skaya, L. G., Khripunov, A. K., & Tkachenko, A. A. (2010). Anisotropic swelling and mechanical behavior of composite bacterial cellulose–poly(acrylamide or acrylamide–sodium acrylate) hydrogels. *Journal of the Mechanical Behavior of Biomedical Materials*, *3*(1), 102–111.

Chang, C. H., Kuo, T. F., Lin, C. C., Chou, C. H., Chen, K. H., Lin, F. H., et al. (2006). Tissue engineering-based cartilage repair with allogenous chondrocytes and gelatin-chondroitin-hyaluronan tri-copolymer scaffold: A porcine model assessed at 18, 24, and 36 weeks. *Biomaterials*, *27*(9), 1876–1888.

Cheung, H.-Y., Lau, K. T., Lu, T. P., & Hui, D. (2007). A critical review on polymer-based bio-engineered materials for scaffold development. *Composites Part B: Engineering*, *38*(3), 291–300.

Chung, C., & Burdick, J. A. (2008). Engineering cartilage tissue. *Advanced Drug Delivery Reviews*, *60*(2), 243–262.

Chung, C., Erickson, I. E., Mauck, R. L., & Burdick, J. A. (2008). Differential behavior of auricular and articular chondrocytes in hyaluronic acid hydrogels. *Tissue Engineering Part A*, *14*(7), 1121–1131.

Chung, C., Mesa, J., Randolph, M. A., Yaremchuk, M., & Burdick, J. A. (2006). Influence of gel properties on neocartilage formation by auricular chondrocytes photoencapsulated in hyaluronic acid networks. *Journal of Biomedical Materials Research Part A*, *77A*(3), 518–525.

Clark, M., & Kiser, P. (2009). In situ crosslinked hydrogels formed using Cu(I)-free Huisgen cycloaddition reaction. *Polymer International*, *58*(10), 1190–1195.

Crescenzi, V., Cornelio, L., Di Meo, C., Nardecchia, S., & Lamanna, R. (2007). Novel hydrogels via click chemistry: Synthesis and potential biomedical applications. *Biomacromolecules*, *8*(6), 1844–1850.

Hu, X., Li, D., Zhou, F., & Gao, C. (2011). Biological hydrogel synthesized from hyaluronic acid, gelatin and chondroitin sulfate by click chemistry. *Acta Biomaterialia*, *7*(4), 1618–1626.

Hu, X. H., Zhou, J., Zhang, N., Tan, H. P., & Gao, C. Y. (2008). Preparation and properties of an injectable scaffold of poly(lactic-co-glycolic acid) microparticles/chitosan hydrogel. *Journal of the Mechanical Behavior of Biomedical Materials*, *1*(4), 352–359.

Itoa, T., Yeo, Y., Highleya, C. B., Bellasa, E., Benitezb, A. C., & Kohane, D. S. (2007). Kohanec The prevention of peritoneal adhesions by in-situ cross-linking hydrogels of hyaluronic acid and cellulose derivatives. *Biomaterials*, *28*(6), 975–983.

Jha, A. K., Malik, M. S., Farach-Carson, M. C., Duncan, R. L., & Jia, X. Q. (2010). Hierarchically structured, hyaluronic acid-based hydrogel matrices via the covalent integration of microgels into macroscopic networks. *Soft Matter*, *6*(20), 5045–5055.

Klein, T. J., Malda, J., Sah, R. L., & Hutmacher, D. W. (2009). Tissue engineering of articular cartilage with biomimetic zones. *Tissue Engineering Part B: Reviews*, *15*(2), 143–157.

Kogan, G., Šoltés, L., Stern, R., & Gemeiner, P. (2006). Hyaluronic acid: A natural biopolymer with a broad range of biomedical and industrial applications. *Biotechnology Letters*, *29*(1), 17–25.

Kolb, H. C., Finn, M. G., & Sharpless, K. B. (2001). Click chemistry: Diverse chemical function from a few good reactions. *Angewandte Chemie International Edition*, *40*(11), 2004–2021.

Lee, J., Tae, G., Kim, Y. H., Park, I. S., Kim, S. H., & Kim, S. H. (2008). The effect of gelatin incorporation into electrospun poly(L-lactide-co-epsilon-caprolactone) fibers on mechanical properties and cytocompatibility. *Biomaterials*, *29*(12), 1872–1879.

Liu, L., Xu, X., Guo, S. A. R., & Han, W. (2009). Synthesis and self-assembly of chitosan-based copolymer with a pair of hydrophobic/hydrophilic grafts of polycaprolactone and poly(ethylene glycol). *Carbohydrate Polymers*, *75*(3), 401–407.

Liu, Y. L., Hsieh, C. Y., & Chen, Y. W. (2006). Thermally reversible cross-linked polyamides and thermo-responsive gels by means of Diels–Alder reaction. *Polymer*, *47*(8), 2581–2586.

Lu, J. X., Flautre, B., Anselme, K., Hardouin, P., Gallur, A., Descamps, M., et al. (1999). Role of interconnections in porous bioceramics on bone recolonization in vitro and in vivo. *Journal of Materials Science – Materials in Medicine*, *10*(2), 111–120.

Matsiko, A., Levingstone, T. J., O'Brien, F. J., & Gleeson, J. P. (2011). Addition of hyaluronic acid improves cellular infiltration and promotes early-stage chondrogenesis in a collagen-based scaffold for cartilage tissue engineering. *Journal of the Mechanical Behavior of Biomedical Materials*, *11*, 41–52.

Munic, E. C., & Geustens, G. (2001). Polyacrylamide hydrogels and semi-interpenetrating networks(IPNs) with poly(N-isopropylacrylamide): Mechanical properties by measure of compressive elastic modulus. *Journal of Materials Science – Materials in Medicine*, *12*(10–12), 879–881.

Nimmo, C. M., Owen, S. C., & Shoichet, M. S. (2011). Diels–Alder click cross-linked hyaluronic acid hydrogels for tissue engineering. *Biomacromolecules*, *12*(3), 824–830.

Palumbo, F. S., Pitarresi, G., Fiorica, C., Matricardi, P., Albanese, A., & Giammona, G. (2012). In situ forming hydrogels of new amino hyaluronic acid/benzoyl-cysteine derivatives as potential scaffolds for cartilage regeneration. *Soft Matter*, *8*(18), 4918–4927.

Rice, M. A., Homier, P. M., Waters, K. R., & Anseth, K. S. (2008). Effects of directed get degradation and collagenase digestion on the integration of neocartilage produced by chondrocytes encapsulated in hydrogel carriers. *Journal of Tissue Engineering and Regenerative Medicine*, *2*(7), 418–429.

Ruhela, D., Riviere, K., & Szoka, F. C., Jr. (2006). Efficient synthesis of an aldehyde functionalized hyaluronic acid and its application in the preparation of hyaluronan-lipid conjugates. *Bioconjugate Chemistry*, *17*(5), 1360–1363.

Steward, A. J., Liu, Y. X., & Wagner, D. R. (2011). Engineering cell attachments to scaffolds in cartilage tissue engineering. *JOM Journal of the Minerals Metals and Materials Society*, *63*(4), 74–82.

Stoddart, M. J., Grad, S., Eglin, D., & Alini, M. (2009). Cells and biomaterials in cartilage tissue engineering. *Regenerative Medicine*, *4*(1), 81–98.

Stoop, R. (2008). Smart biomaterials for tissue engineering of cartilage. *Injury – International Journal of the Care of the Injured*, *39*(Suppl. 1), 77–87.

Sun, J. Y., Zhao, X., Illeperuma, W. R. K., Chaudhuri, O., Oh, K. H., Mooney, D. J., et al. (2012). Highly stretchable and tough hydrogels. *Nature*, *489*(7414), 133–136.

Tamura, G., Shinohara, Y., Tamura, A., Sanada, Y., Oishi, M., Akiba, I., et al. (2012). Dependence of the swelling behavior of a pH-responsive PEG-modified nanogel on the cross-link density. *Polymer Journal*, *44*(3), 240–244.

Tan, H., Rubin, J. P., & Marra, K. G. (2011). Direct synthesis of biodegradable polysaccharide derivative hydrogels through aqueous diels–alder chemistry. *Macromolecular Rapid Communications*, *32*(12), 905–911.

Tang, Y. J., Sun, J., Fan, H. S., & Zhang, X. D. (2012). An improved complex gel of modified gellan gum and carboxymethyl chitosan for chondrocytes encapsulation. *Carbohydrate Polymers*, *88*(1), 46–53.

Tasdelen, M. A. (2011). Diels–Alder "click" reactions: Recent applications in polymer and material science. *Polymer Chemistry*, *2*(10), 2133.

Temenoff, J. S., & Mikos, A. G. (2000). Review: Tissue engineering for regeneration of articular cartilage. *Biomaterials*, *21*(5), 431–440.

Toh, W. S., Lim, T. C., Kurisawa, M., & Spector, M. (2012). Modulation of mesenchymal stem cell chondrogenesis in a tunable hyaluronic acid hydrogel microenvironment. *Biomaterials*, *33*(15), 3835–3845.

Toh, W. S., Spector, M., Lee, E. H., & Cao, T. (2011). Biomaterial-mediated delivery of microenvironmental cues for repair and regeneration of articular cartilage. *Molecular Pharmaceutics*, *8*(4), 994–1001.

Tominaga, T., Sano, K.-I., Kikuchi, J., Mitomo, H., Ijiro, K., & Osada, Y. (2012). Hydrophilic double-network polymers that sustain high mechanical modulus under 80% humidity. *ACS Macro Letters*, *1*(3), 432–436.

Vinatier, C., Mrugala, D., Jorgensen, C., Guicheux, J., & Noel, D. (2009). Cartilage engineering: A crucial combination of cells, biomaterials and biofactors. *Trends in Biotechnology*, *27*(5), 307–314.

Wei, H. L., Yang, Z., Chu, H. J., Zhu, J., Li, Z. C., & Cui, J. S. (2010). Facile preparation of poly(N-isopropylacrylamide)-based hydrogels via aqueous Diels–Alder click reaction. *Polymer*, *51*(8), 1694–1702.

Wei, H. L., Yang, Z., Zheng, L. M., & Shen, Y. M. (2009). Thermosensitive hydrogels synthesized by fast Diels–Alder reaction in water. *Polymer*, *50*(13), 2836–2840.

Yigit, S., Sanyal, R., & Sanyal, A. (2011). Fabrication and functionalization of hydrogels through "click" chemistry. *Chemistry: An Asian Journal*, *6*(10), 2648–2659.

Zhou, C. J., & Wu, Q. L. (2011). A novel polyacrylamide nanocomposite hydrogel reinforced with natural chitosan nanofibers. *Colloids and Surfaces B – Biointerfaces*, *84*(1), 155–162.

Zhou, C., Wu, Q., Yue, Y., & Zhang, Q. (2011). Application of rod-shaped cellulose nanocrystals in polyacrylamide hydrogels. *Journal of Colloid and Interface Science*, *353*(1), 116–123.